

Hard X-ray Microbeam Experiment at the Tristan Main Ring Test Beamline of the KEK

Y. Suzuki,^a N. Kamijo,^b S. Tamura,^b K. Handa,^c A. Takeuchi,^d S. Yamamoto,^e H. Sugiyama,^e K. Ohsumi^e and M. Ando^e

^aAdvanced Research Laboratory, Hitachi Ltd, Hatoyama, Saitama 350-03, Japan, ^bOsaka National Research Institute, AIST, Ikeda, Osaka 563, Japan, ^cRitsumeikan University, Noji Kusatsu, Shiga 525-77, Japan, ^dTsukuba University, Tsukuba, Ibaraki 305, Japan, and ^ePhoton Factory, National Laboratory for High Energy Physics, Tsukuba, Ibaraki 305, Japan. E-mail: suzuki@harl.hitachi.co.jp

(Received 13 November 1996; accepted 26 November 1996)

A hard X-ray microbeam with zone-plate optics has been tested at the MR-BW-TL beamline on the Tristan main ring of the KEK, and preliminary experiments on scanning microscopy have also been performed. A sputtered-sliced Fresnel zone plate with an Au core and Ag/C multilayer is used as an X-ray focusing device. The outermost zone width of the zone plate is 0.25 μm . A focused spot size of $\sim 0.5 \mu\text{m}$ has been achieved at an X-ray energy of 8.54 keV. In a scanning X-ray microscopy experiment, test patterns with submicrometer fine structure have been clearly resolved.

Keywords: microbeams; zone plates; scanning microscopy.

1. Introduction

The X-ray microbeam is considered to be a key technology for third-generation high-brilliance synchrotron radiation sources. Achieving an X-ray microprobe with submicrometer spot size in the hard X-ray region is expected to add a new dimension to various X-ray analysis methods. Hard X-ray microbeam projects are planned or in progress at many synchrotron radiation facilities. Many types of optical devices, including total reflection mirrors (Hayakawa, Iida, Aoki & Gohshi, 1989; Suzuki & Uchida, 1992; Iida & Noma, 1993; Yang, Rivers, Schidkamp & Eng, 1995), multilayer mirrors (Underwood, Thompson, Wu & Giauque, 1988), X-ray capillaries (Bilderback, Hoffman & Thiel, 1994), Bragg Fresnel lenses (Basov *et al.*, 1991; Kuznetsov, Snigireva, Snigirev, Engström & Riekel, 1994; Erko *et al.*, 1994; Snigirev *et al.*, 1995; Snigirev, 1995) and Fresnel zone plates (FZP) (Saitoh *et al.*, 1989; Bionta *et al.*, 1989, 1990; Bionta, Skulina & Weinberg, 1994; Lai *et al.*, 1992; Yun *et al.*, 1992; Kamijo, Tamura, Suzuki & Kihara, 1995a,b; Tamura, Ohtani & Kamijo, 1994), are used to generate the microfocus X-ray beam. At the ESRF, a hard X-ray microbeam generated by a Bragg Fresnel lens has been extensively studied. A spatial resolution of 0.8 μm has already been achieved for 14.6 keV X-rays by one-dimensional focusing with a linear Bragg Fresnel lens (Kuznetsov *et al.*, 1994), and a focused 0.7 μm spot has been generated with a circular Bragg Fresnel lens for 7.6 keV X-rays (Snigirev *et al.*, 1995). Hard X-ray microprobe experiments with Fresnel zone plates fabricated by lithography-based techniques have been performed at the NSLS, and a focused spot size of 0.6–0.7 μm has been obtained at an X-ray energy of 8 keV (Yun *et al.*, 1992).

We have developed X-ray microbeam optics with spherical total-reflection mirrors (Suzuki & Uchida, 1992) and optics with sputtered-sliced FZP (Kamijo *et al.*, 1995a,b). X-ray focusing properties were evaluated at the Photon Factory bending-magnet beamline, and a nominal spatial resolution of $\sim 1 \mu\text{m}$ has already been achieved both with mirror optics (Suzuki & Uchida, 1992) and FZP optics (Kamijo *et al.*, 1995b). However, synchrotron radiation from a normal bending magnet of the Photon Factory 2.5 GeV storage ring is insufficient for microbeam experiments because of the low photon flux and high beam emittance. The photon flux of a focused X-ray beam is limited by the source brilliance because of emittance conservation in optical systems for X-rays. A high-brilliance X-ray source is indispensable for X-ray microprobes. We have attempted to generate a hard X-ray microbeam with submicrometer spot size at the Tristan main ring test beamline. In this paper we describe the results of an X-ray focusing test in which a sputtered-slice FZP was used. We also discuss its application to scanning X-ray microscopy.

2. Experimental set-up

2.1. X-ray source

The Tristan main ring at the National Laboratory for High Energy Physics (KEK) is an electron-positron colliding ring constructed for experiments on elementary particles. Its circumference is 3 km; the maximum beam energy is 31 GeV. The ring was modified to operate as a high-brilliance synchrotron light source. A planar-type 120-pole undulator with a magnetic period of 4.5 cm and maximum K value of 1.1 was installed in the straight section of

the Tristan main ring. The storage ring was operated at 8 GeV in multibunch mode for the microbeam experiment. The stored electron beam current was 2–15 mA during the experiment. Details of the storage ring and undulator will be described elsewhere (Yamamoto, Sugiyama, Tsuchiya & Shioya, 1997).

2.2. Beamline

A schematic diagram of the experimental set-up is shown in Fig. 1. Undulator radiation passing through double graphite heat absorbers (each 0.1 mm thick) and double beryllium windows (each 0.2 mm thick) is monochromatized with a liquid-nitrogen-cooled Si 220 double-crystal monochromator, and the X-ray energy is fixed at 8.54 keV. The K value of the undulator is tuned by changing the magnet gap as the output flux from the monochromator reaches maximum. The third beryllium window (0.2 mm thick), located between the first and second crystals of the monochromator, separates the vacuum from atmospheric pressure. Finally, the monochromatic X-ray beam impinges on an X-ray focusing device in air. The distance between the light source and the experimental station is ~ 100 m. A cross slit is placed between the first and second crystals of the monochromator. The cross slit is used as a pseudo point source for the microbeam experiment, and a demagnified image of the cross slit is generated at the focal point to generate a microfocus X-ray beam. The distance between the cross slit and the X-ray focusing device is ~ 16 m. Details of the beamline and monochromator system will be published elsewhere by other authors (Sugiyama, Zhang, Higashi, Arakawa & Ando, 1997).

2.3. Sputtered-sliced Fresnel zone plate

A sputtered-sliced FZP fabricated by Kamijo & Tamura (Kamijo *et al.*, 1995a; Tamura *et al.*, 1994) is used as the X-ray focusing device. The fabrication process for the sputtered-sliced FZP was developed by Saitoh *et al.* (1989). The sputtered-sliced FZP used in this experiment consists of alternate opaque and transparent multilayer zones constructed by magnetron sputtering. Fifty Ag/C concentric multilayer structures are deposited onto an Au wire substrate of diameter $47 \mu\text{m}$, and the film thickness

(zone width) of the first inner layer is set to $0.4 \mu\text{m}$ and the outermost layer to $0.25 \mu\text{m}$. The diameter of the FZP is $80 \mu\text{m}$ under these conditions. The diffraction limit for spatial resolution determined by the width of the outermost zone ($0.25 \mu\text{m}$) is $0.3 \mu\text{m}$ for the first-order focus.

After deposition, the wire sample is sliced normal to the wire axis onto a plate. Finally, the FZP is thinned by mechanical polishing. When the thickness of the FZP is more than $10 \mu\text{m}$, the FZP operates as an amplitude-modulating zone plate, and the efficiency of the first-order diffraction is less than $1/\pi^2$ ($\sim 10\%$). When the FZP is thinned to less than $10 \mu\text{m}$, the zone plate becomes a phase-modulating zone plate (Bionta *et al.*, 1989, 1990, 1994), and the theoretical limitation of the first-order diffraction efficiency increases to 40%. The thickness of the FZP used in this experiment is estimated to be ~ 8 – $9 \mu\text{m}$. The diffraction efficiency is measured by comparing the flux density of X-rays incident on the FZP with the intensity of the focused beam. The measured efficiency of the first-order diffraction is $\sim 10\%$ at an X-ray energy of 8 keV. The FZP has a central stop zone ($47 \mu\text{m}$ -diameter gold core). Taking the annular aperture of the FZP into account, the intrinsic diffraction efficiency achieved by the zoned area is estimated to be $\sim 16\%$. This value is apparently larger than the theoretical limitation of the first-order diffraction efficiency for the amplitude-contrast FZP. Therefore, this FZP is considered to be a phase-shifted FZP.

The measured focal length is ~ 146 mm at an X-ray energy of 8.54 keV. In this experiment a demagnified image of the X-ray source is formed by the FZP to generate a microfocus X-ray beam. When the cross slit placed between the first and second crystals of the monochromator is used as a point-like X-ray source, the magnification (M) is defined by the equation $M = f/L$, where f (146 mm) is the focal length of the FZP and L (16 m) is the distance between the source and FZP. The slit width used in this experiment is estimated to be $\sim 50 \mu\text{m}$. When the slit width is $50 \mu\text{m}$, a focused spot size of $0.5 \mu\text{m}$ can be derived by geometrical optics. An order-sorting aperture (OSA), a $20 \mu\text{m}$ -diameter pinhole made of 0.2 mm-thick Ta plate, is used for selecting the first-order diffraction. The diameter of the order-sorting aperture is optimized so as to maximize

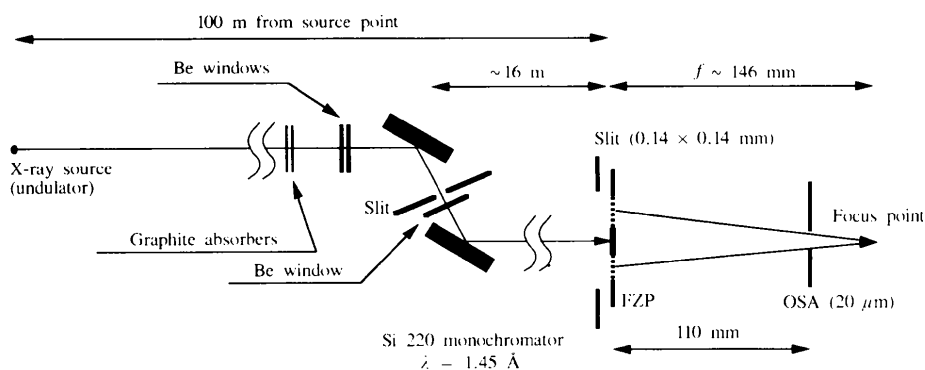


Figure 1

The optical system (OSA: order sorting aperture; FZP: sputtered-sliced Fresnel zone plate).

the distance between the aperture and focus point. The exact values for optimization were an order-sorting aperture diameter of $21\ \mu\text{m}$ and a maximum distance between the aperture and focal point of $40\ \text{mm}$.

2.4. Scanning X-ray microscopy instruments

The FZP, bonded onto a graphite plate ($1\ \text{mm}$ thick), is mounted onto a manipulator. A cross slit ($0.14 \times 0.14\ \text{mm}$) is placed just in front of the FZP to reduce background noise. The intensity of the monochromator output beam is monitored by an ionization chamber (air, $1\ \text{atm}$), and the intensity of the focused X-ray beam is measured with an ionization chamber or an NaI scintillation counter. Focused beam profiles are measured by knife-edge scans. The knife-edge, which is actually a gold wire of diameter $50\ \mu\text{m}$, is scanned with a translation stage driven by a stepping motor. The minimum step of the scanner is $0.025\ \mu\text{m}$. The line-spread function of the optical system is derived from the numerical differential of the measured knife-edge scan profiles. A scanning X-ray microscopy experiment is performed by raster-scanning the sample with the same translation stage; the two-dimensional measurement data are displayed as false-colour images.

3. Results

3.1. X-ray focusing properties

The cross slit between the first and second crystals of the monochromator is used as a pseudo point source for the X-ray focusing experiment. The focused beam profile measured by knife-edge scanning is shown in Fig. 2. The knife-edge was scanned in $0.125\ \mu\text{m}$ steps and the focused

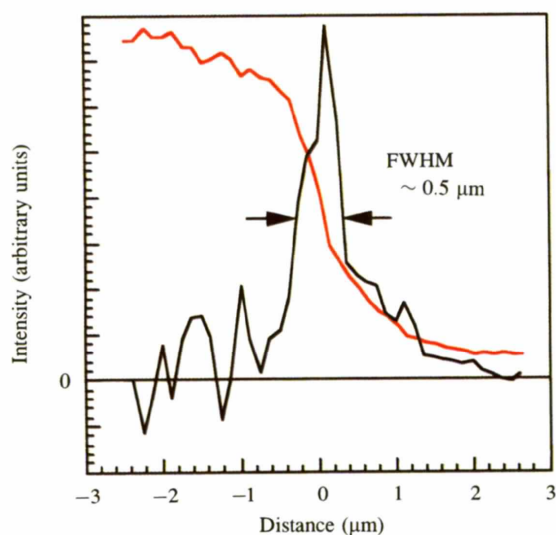
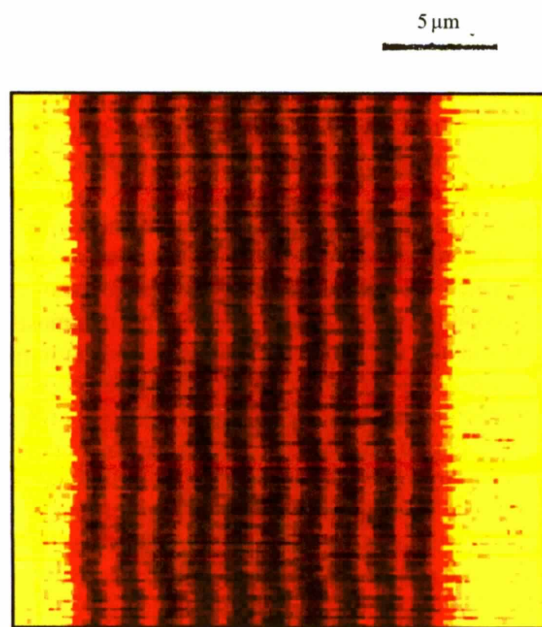


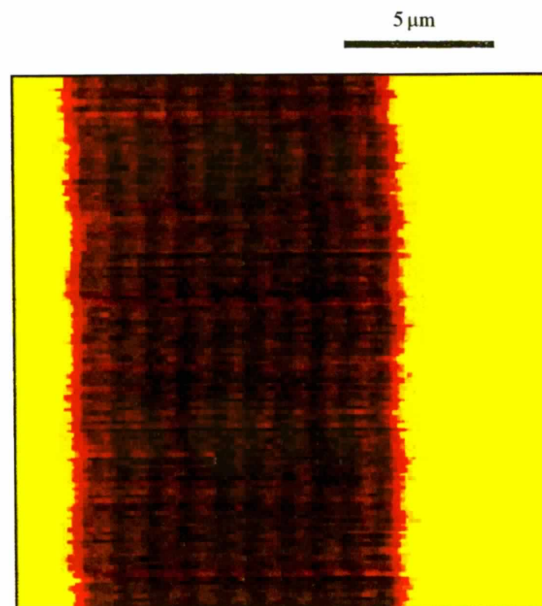
Figure 2

Focused beam profile measured by horizontal knife-edge scanning. The red line represents raw intensity data from an edge scan; the black line is the numerical derivative. The X-ray energy is $8.54\ \text{keV}$. The cross slit between the first and second crystals of the monochromator is used as a pseudo point source.

beam profile was simply derived by a numerical finite differentiation of the measured edge profile. A spot size (spatial resolution) of $\sim 0.5\ \mu\text{m}$ full width at half maximum (FWHM) was achieved. This spot size is very close to the diffraction-limited resolution of the FZP ($0.3\ \mu\text{m}$). Therefore, the FZP used in this experiment is considered to be very near to that of the ideal zone plate.



(a)



(b)

Figure 3

Scanning microscopic images of test patterns. (a) $0.9\ \mu\text{m}$ line and $0.9\ \mu\text{m}$ space pattern, (b) $0.6\ \mu\text{m}$ line and $0.6\ \mu\text{m}$ space. The X-ray energy is $8.54\ \text{keV}$. Two-dimensional images of 128×128 pixels are acquired by raster-scanning the sample. Pixel size: (a) $0.2\ \mu\text{m}$, (b) $0.15\ \mu\text{m}$. Dwell time: $0.2\ \text{s pixel}^{-1}$.

The FZP was not a practical device in the bending magnet beamline of the Photon Factory 2.5 GeV storage ring because of low efficiency and small numerical aperture. However, by using the high-brilliance undulator radiation from the Tristan main ring, a practical hard X-ray microprobe was achieved. When the demagnified image of the undulator source point is formed by the FZP, the focused beam size measured by edge-scanning was $1.4\ \mu\text{m}$ FWHM, and the flux density of the focused X-ray beam measured with the ionization chamber was $\sim 1 \times 10^6\ \text{photons s}^{-1}\ \mu\text{m}^{-2}$ for a 10 mA stored current. This beam intensity is sufficient for the scanning microscopy experiment, and test patterns with submicrometer fine structure have been clearly resolved in preliminary experiments.

3.2. Scanning microscopy experiment

A mask pattern for X-ray lithography was used as a resolution test pattern for evaluating the performance of the scanning microscope. It has periodic line and space patterns made of $1\ \mu\text{m}$ -thick gold deposited on a composite membrane of boron nitride and polyimide resin. The focused beam size used in the scanning microscopy experiment was slightly larger than that shown in Fig. 2 because of the width of the slit opening used as the pseudo point source. The probe size was estimated to be $\sim 0.9\ \mu\text{m}$ (FWHM). The transmittance of the $1\ \mu\text{m}$ -thick gold film is $\sim 71\%$ for 8.54 keV X-rays. Therefore, absorption contrast is very low in this experiment. However, patterns of $0.9\ \mu\text{m}$ lines and $0.9\ \mu\text{m}$ spaces were clearly resolved, as shown in Fig. 3(a). Fine structures of $0.6\ \mu\text{m}$ lines and $0.6\ \mu\text{m}$ spaces were also resolved, as shown in Fig. 3(b). The amplitude transfer function in the measured images was $\sim 30\%$ for $0.9\ \mu\text{m}$ line/space patterns and 14% for $0.6\ \mu\text{m}$ line/space patterns.

4. Conclusions

X-ray microprobe experiments performed at the Tristan main ring test beamline in the National Laboratory for High Energy Physics achieved a focused beam size of $\sim 0.5\ \mu\text{m}$ at an X-ray energy of 8.54 keV by using a sputtered-sliced Fresnel zone plate as an X-ray focusing device. A high-brilliance undulator X-ray source made it possible to generate a micrometer-sized high-intensity hard X-ray microprobe. A flux density of $1 \times 10^6\ \text{photons s}^{-1}\ \mu\text{m}^{-2}$ was obtained for a 10 mA stored current. In scanning microscopy with the microfocus X-ray beam, fine resolution $0.6\ \mu\text{m}$ line/space test patterns were resolved.

The authors would like to express much appreciation to all the members of the Tristan super light facility and the accelerator group of the Tristan for their help in the experiment. They are also grateful to Dr S. Aoki for his valuable advice. This study has been performed under the approval of the Tristan-MR Committee (proposal No. MR95A).

References

- Basov, Y. A., Pravdivtseva, T. L., Snigirev, A. A., Belakhovsky, M., Dhez, P. & Freund, A. (1991). *Nucl. Instrum. Methods*, **A308**, 363–366.
- Bilderback, D. H., Hoffman, S. A. & Thiel, D. J. (1994). *Science*, **263**, 201–203.
- Bionta, R. M., Ables, E., Clamp, O., Edwards, O. D., Gabriele, P. C., Makowicki, D., Ott, L. L., Skulina, K. M. & Thomas, N. (1989). *Proc. SPIE*, **1160**, 12–18.
- Bionta, R. M., Ables, E., Clamp, O., Edwards, O. D., Gabriele, P. C., Miller, K., Ott, L. L., Skulina, K. M., Tilley, R. & Viada, T. (1990). *Opt. Eng.* **29**, 576–580.
- Bionta, R. M., Skulina, K. M. & Weinberg, J. (1994). *Appl. Phys. Lett.* **64**, 945–947.
- Erko, A., Agafonov, Y., Panchenko, L. A., Yakshin, A., Chevallier, P., Dhez, O. & Legrand, F. (1994). *Opt. Commun.* **106**, 146–150.
- Hayakawa, S., Iida, A., Aoki, S. & Gohshi, Y. (1989). *Rev. Sci. Instrum.* **60**, 2452–2455.
- Iida, A. & Noma, T. (1993). *Nucl. Instrum. Methods*, **B82**, 129–138.
- Kamijo, N., Tamura, S., Suzuki, Y. & Kihara, H. (1995a). *Rev. Sci. Instrum.* **66**, 2132–2134.
- Kamijo, N., Tamura, S., Suzuki, Y. & Kihara, H. (1995b). *Photon Fact. Act. Rep.* **94**, 165.
- Kuznetsov, S. M., Snigireva, I. I., Snigirev, A. A., Engström, P. & Riekel, C. (1994). *Appl. Phys. Lett.* **65**, 827–829.
- Lai, B., Yun, W. B., Legnini, D., Xiao, Y., Crzas, J., Viccaro, P. J., White, V., Denton, D., Cerrina, F., Di Fabrizio, E., Grella, L. & Baciocchi, M. (1992). *Appl. Phys. Lett.* **61**, 1877–1879.
- Saitoh, K., Inagawa, K., Kohra, K., Hayashi, C., Iida, A. & Kato, N. (1989). *Rev. Sci. Instrum.* **60**, 1519–1523.
- Snigirev, A. (1995). *Rev. Sci. Instrum.* **66**, 2053–2058.
- Snigirev, A., Snigireva, I., Engström, P., Lequien, S., Suvorov, A., Hartman, Ya., Chevallier, P., Idir, M., Legrand, F., Soullie, G. & Engrand, S. (1995). *Rev. Sci. Instrum.* **66**, 1461–1463.
- Sugiyama, H., Zhang, X., Higashi, Y., Arakawa, K. & Ando, M. (1997). In preparation.
- Suzuki, Y. & Uchida, F. (1992). *Rev. Sci. Instrum.* **63**, 578–581.
- Tamura, S., Ohtani, K. & Kamijo, N. (1994). *Appl. Surf. Sci.* **79/80**, 514–518.
- Underwood, J. H., Thompson, A. C., Wu, Y. & Giauque R. D. (1988). *Nucl. Instrum. Methods*, **A266**, 296–302.
- Yamamoto, S., Sugiyama, H., Tsuchiya, K. & Shioya, T. (1997). *J. Synchrotron Rad.* **4**, 54–59.
- Yang, B. X., Rivers, M., Schidkamp, W. & Eng, P. J. (1995). *Rev. Sci. Instrum.* **66**, 2278–2280.
- Yun, W., Lai, B., Legnini, D., Xiao, Y. H., Chrzas, J., Skulina, K. M., Bionta, R. M., White, V. & Cerrina, F. (1992). *SPIE J.* **1740**, 117–129.